AIMS Materials Science, 8(5): 685–697.
DOI: 10.3934/matersci.2021041
Received: 17 July 2021
Accepted: 07 September 2021
Published: 09 September 2021

http://www.aimspress.com/journal/Materials

Research article

Open die forging process simulation: a simplified industrial approach based on artificial neural network

Andrea Di Schino*

Department of Engineering, University of Perugia, 06125 Perugia, Italy

* **Correspondence**: Email: andrea.dischino@unipg.it.

Abstract: Simulations by Finite element analysis (FEM) of open die forging process related to different configurations are quite common in industry to optimize the process. This approach, anyway, is relatively slow to be performed: hence it is not suitable for online optimization of the forging processes. In this paper a simplified approach is proposed aimed to describe the plastic strain at the core of the forged component. The proposed approach takes into account the plastic deformation at the core of the forged component and consists on a thermo-mechanical FEM model implementation allowing to define a set of equations giving as output the plastic strain at the core of the piece as a function of the forging parameters. An Artificial Neural Network (ANN) is trained and tested aimed to relate the equation coefficients with the forging to obtain the behavior of plastic strain at the core of the piece.

Keywords: open die forging; artificial neural network; fast simulator; process optimization

1. Introduction

Forged steels are a quite promising material family, both from a scientific and commercial point of view, based on the several and quite different applications they can be devoted to [1]. In this framework, it is quite important to focus on the relations between mechanical properties and microstructural features in order to understand how to process the material in order to achieve them [2–6]. Forged materials are widely used in the machining and forming industry [7–9], in automotive sector [10], and in other applications including aerospace, transport, and precision industries [11–13]. In addition, as the energy and power engineering industry grow large-sized

hot-forged products demand has also increased. This includes turbine shafts (water, gas, steam), rotors for wind, and gas power generators [14]. Based on data from EUROFORGE (an organization that associates European production associations, including the Polish Forge Association), the volume of forged products has been growing steadily, and in 2021 it will reach over 10 million tons. The global forging market is likely to grow significantly at a CAGR (Compound Annual Growth Rate) of close to 8%, reaching USD 111.1 billion by 2020, according to Technavio's latest report [14].

In all the above applications, forged steels are used based on a requirement asking for increasing manufacturing economic efficiency and improved mechanical properties, such as high strength, wear resistance, hardness, and toughness [15,16].

Free forging is the more common forging technology commonly adopted to forge heavy charge materials in short production runs. High-pressure hydraulic forging presses are on the other hand used in open die forging of heavy steel forgings (carbon, alloy, high-alloy, stainless and other steels). Open die forging is an incremental forging technology mainly adopted to manufacture large components asking for improved tensile properties and toughness behavior together with reliability of the forged parts [17]. In the steel industry, there is a strong need to produce large components characterized by high weight, calling for high press loads. Such components can be spindles, rolling mills rolls as well large turbine shafts and nuclear reactor vessels [18,19]. In the open die forging process the workpiece is processed using flat or shaped dies. The piece is subjected to a high temperature plastic deformation. Both the component geometry and internal properties are affected by the above process [20].

Cavities and porosities amount (coming from the casting process) is reduced by forging process. This allows to manufacture almost defect free components thus assuring homogeneous plastic strain in the piece [21,22]. The open die forging process quality is affected by many different parameters (e.g., die width and shape, ingot shape and size, temperature gradient, pass schedule, and so on [23]). In order to achieve the requirements in term of geometric tolerance and internal quality, it is common practice to set up an adequate pass schedule previously verified by means of numerical simulations. In order to do that, in the case of forging sequence design and optimization, it is necessary to simulate many different configurations with the aim to identify the best solution. FEM is one of the most commonly adopted approach. Anyway, it is well known that such approach requires significant efforts in terms of both computational resources and time [24,25].

Following to the above limitation, it is useful to develop fast calculation models of the open die forging process allowing to perform a rapid calculation of material properties during the layout of the process as well for the online monitoring of the process.

In the past, some authors dedicated to the development of fast models oriented to open die forging process optimization [26–30]. The common idea at the base of the above works was to develop process models able to combine data from online measurements and a simplified plasto-mechanical model for the forecasting of the equivalent strain, strain rate, and the temperature in the core of the forged piece. The final aim of such models is to optimize the stretching forging not only from a geometric point of view but also in terms of final microstructure, internal quality (e.g., casting porosity closure), working temperature to avoid phase transformation during the mechanical processing. Kim et al. [27] developed forging pass schedule algorithms based on artificial neural networks (ANN) are mainly oriented to calculate the optimum number of passes and reduction in each pass to economize power and minimize the forging cycle time. The algorithms were trained on the experimental data from pilot and full-scale industrial forging.

Starting from the approach reported in [28–30], an innovative formulation based on Artificial Neural Networks (ANN) [31,32] is here proposed aimed to quickly (fraction of a second) and

correctly evaluate the plastic strain at the core of the forged component. Starting from the coefficients for the new analytical model, a neural network has been implemented and trained using analytic coefficients. This allows to calculate the plastic strain occurring during the forging process. The correct evaluation of plastic strain at the core fiber of the forged steel component is a key parameter to be considered in a tool which targets at the internal integrity of the material or the final microstructure optimization.

2. Materials and methods

2.1. FEM model for open-die forging of 42CrMo4 steel grade

The open die forging of large components is a very complex issue characterized by a sequence of several forging operations including upsetting, cogging, drawing. Furnace soaking to reheat the pieces between deformation steps also needs to be taken into account. In such complex process quite important is the ability to predict microstructure evolution with the aim to target the final target properties. In the stretching forging process, the pass sequence is roughly square or round to octagon to round, where the reduction ratio only varies every second pass. In the considered pass sequence, the round is forged to an oval section with a given height reduction, turned 90°, and then forged again with the same reduction and same bite ratio, producing a square cross-section. The final achieved square bar is now forged into an octagonal bar. This represents an intermediate shape between square and round. As a final step. the round bar is manufactured in single and consequent passes by deforming the octagonal bar. The octagonal bar has a greater cross-sectional area than the final round bar. The round bar is then finished in a round-contoured die during the finishing passes. Simulation of the stretching forging process of a 42CrMo4 steel has been performed by FE model developed using the commercial code MSC.Marc. Such code is well known for being characterized by a high accuracy tool for closed and open die forging process simulation [33–35]. The strokes start in the central part of the piece and proceed until the 4^{th}. Accurate predictions from the model calls for proper material models able to describe the flow stress. This is why, laboratory compression tests are usually performed by means of Gleeble on cylindrical specimens with different temperatures, strains, strains rates, post deformation holding times to characterize the flow stress, static recrystallization and grain size evolution during forging. The rheology has been modelled following [36,37] model.

At a first stage, some forging key parameters have been chosen in order to simulate the deformation process, such as: ingot diameter D, contact die length Sb0, forged piece temperature, percentage reduction. The chosen die has a flat shape, and the numerical values of the parameters adopted to implement the FEM model are shown in Table 1, which corresponds to about 600 simulations after DOE. The DOE considered method is based on a linear model with an additional term aimed to take into account possible interaction between factors.

Table 1. Parameters of FEM simulation for stretching forging process for round ingot.

Forging parameter	Minimum value	Maximum value	Step
Temperature (°C)	800	1200	100
Sb_0 (mm)	150	750	150
Reduction (%)	5.0	25.0	2.5
ΔSb_0 (%) (Pitch (%) respect Sb_0)	10 (90%)	50 (50%)	(20%)
Ingot initial diameter (mm)	300	1500	300

The model was implemented considering a double symmetry in longitudinal and radial directions and a constraint in order to take into account the presence of the manipulator during the forging process. Calculations were carried out considering isothermal condition, without exchange between ingot and external environment and tools in order to separate the thermal effect from the mechanical one on the plastic strain at the core of the ingot.

2.2. Analytical model for open die process simulation

A preliminary analysis of FEM results in terms of plastic strain at the core of the forged piece (Figure 1) has been carried out in order to represent the plastic strain at the center of the piece. An example of output of the FEM thermo-mechanical simulation is reported in Figure 2. In such plot the plastic strain evolution as a function of length at 1200 °C, Sb_0 = 300 mm, reduction = 25% is reported. Figure 2 shows how the simulated forging process is characterized by a first stroke with a major contact zone since the material is not yet deformed. The last three strokes follow the Same evolution characterizes the following strokes. In this paper a separation of the strokes has been performed aimed to distinguish each one. This will allow to separately apply the analytical model and the neural network. In addition, since a similar behavior in terms of maximum plastic strain is reported for strokes from 2nd to 4th, only the first and the second strokes are considered in the analysis.

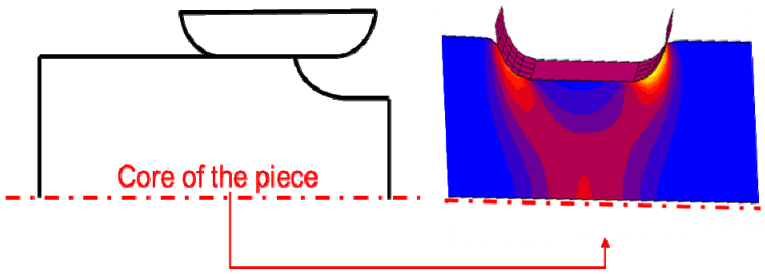

Figure 1. Schematic representation of forged piece simulated; results have been token at the core of the piece in terms of plastic strain as a function of the length.

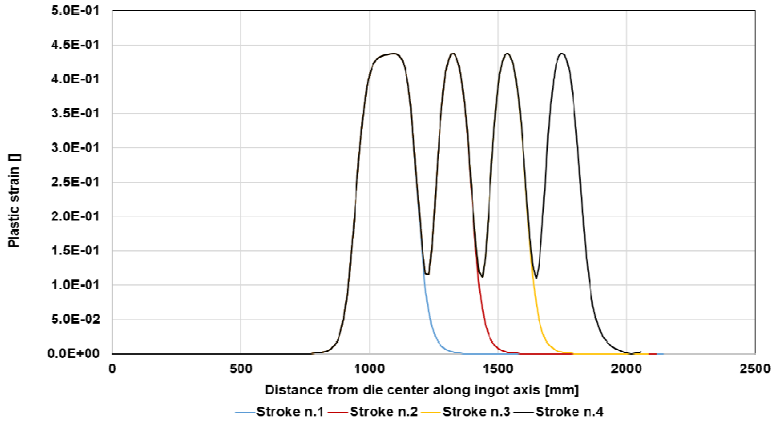

Figure 2. Evolution of plastic strain as a function of length at 1200 °C, Sb_0 = 300 mm, reduction = 25%, ingot diameter equal to 300 mm, pitch 90%.

A double sigmoidal function has been chosen to represent the evolution of the core fiber plastic strain of a single stroke [37–39]. The sum of two hyperbolic tangents (Eq 1) has been implemented in order to better reproduce the plastic strain evolution at the core of the forged piece along the ingot axis. The growth phase and decay phase of plastic strain are described by Eqs 2,3. Eq 1 varies from 0 to 2 and is continuously derivable and defined throughout the Real numbers domain, therefore it can be used without problems in an optimization system.

$$\varepsilon_{tot}^{p} = \mathrm{M}^{*}\left(\tanh\left(\frac{\mathrm{x}-\mathrm{C}_1}{\mathrm{D}_1}\right) + \tanh\left(-\frac{\mathrm{x}-\mathrm{C}_2}{\mathrm{D}_2}\right)\right) \tag{1}$$

$$\varepsilon_{1}^{p} = \tanh\left(\frac{\mathrm{x}-\mathrm{C}_1}{\mathrm{D}_1}\right) \tag{2}$$

$$\varepsilon_{2}^{p} = \tanh\left(-\frac{\mathrm{x}-\mathrm{C}_2}{\mathrm{D}_2}\right) \tag{3}$$

Coefficients in equations 1, 2, 3 represent respectively:

- C1 and C2: middle points of growth and decay phase respectively.
- D1 and D2: slopes of the growth and decay branches of the function.
- M is a multiplier coefficient. The Eq 1 varies in a range between 0 and 2, thus the coefficients M brings the maximum of double-sigmoidal curve to the maximum of plastic strain.

C1, C2, D1, D2 and M have been calculated by fitting of double-sigmoidal model on the FEM results in terms of total equivalent plastic strain along the core fiber for each forging configuration considered in this analysis. The above obtained coefficients do not have an identified mathematical dependence by forging parameters. The fitting of mathematical model as shown by equation 1 to the individual conditions of the forging process could be carried out using a fragmented, look-up table-based approach. This approach has disadvantages due to the required size for the look-up tables and the lack of interpolation capability. The application of neural networks within the control strategy, setup model, and optimization tool has significantly reduced such kind of problems [40]. The obtained coefficients were used to train the proposed neural network.

2.3. Forecasting models based on Artificial Neural Networks (ANNs)

The artificial neural networks (ANNs) is a nonlinear regressive models, allowing the correlation between a set of independent variables and a set of dependent variables.

Neural Networks are mathematical approaches able to learn from empirical data which are collected in some problem domain by approximating sample of it in a data set. This is done without any assumption about the physical laws. This correlation between variables is achieved through a training process during which a data set containing both independent and dependent variables is used to iteratively adapt the internal structure of the neural model to its purpose [41].

Many families of artificial neural networks are known, according to the learning and recall algorithms. The network adopted in this paper belongs to the Multi-Layer Perceptron (MLP) family based on Back Propagation (BP) learning algorithm [42]. Such algorithm turns to the best configuration of the weights. This is achieved by calculating the error between the target and the network response. The Root Mean Squared (RMS) error has been adopted as index of performance both for each single output variable and for the output as a whole.

The performance of the selected approach is strongly dependent on data quality itself. In our case, no data duplication (similarities) or scattering are present in the data. This is guaranteed by the

fact that data are given by results of a FE model and that simulations are defined by means of a DOE. This allow to avoid any correction (elimination of similarities) or filtering action [41,42]. Clustering analysis was carried out in order to define and identify the cluster, and then for the definition of best neural network topology and number of neural networks. The independent variables of ANN are the forging parameters in terms of forged component temperature and diameter, Sb0, fitch, reduction and stroke number while the output is in terms of the coefficients of double-sigmoidal function that models total equivalent plastic strain. Input and output data have been normalized within the range 0 and 1 with a linear function between the minimum and maximum value of each quantity, Table 2.

Each node in ANN is fully connected to the nodes of the following layer (hidden or not) through a sigmoidal transferring function and weights whose value is adapted during the learning phase to encode on them the knowledge of the forging process described by the used dataset [42]. The implemented ANN is composed of 1 bias node and a single hidden layer characterized by 13 hidden nodes, determined by the formula: l = sqrt(p + q + k), considering the smallest hidden layer error.

The initial data, that consisted in about 600 examples, has been divided into three groups:

- Training: about 400 examples
- Validation: about 150 examples
- Test: about 50 examples

The examples have been subdivided considering the three main clusters identified during the data analysis.

Table 2. Normalized values for artificial neural network.

Variable	Min value	Max value	Min normalized value	Max normalized value
Sb_0	75	750	0.1	0.9
Temperature	800	1200	0.1	0.9
Reduction (%)	5	25	0.1	0.9
C_1	−384	−28	0.1	0.9
D_1	19	60	0.1	0.9
C_2	9.5	350	0.1	0.9
D_2	27	60	0.1	0.9
M	0	0.24	0.1	0.9

3. Results and discussion

The comparison between equation 1coefficients calculated by FE model and by ANN related to the 50 examples used for the tests are shown in Figures 3 and 5. The figures show how data groups into three identified cluster. The scatter plot related to the C1 and C2 coefficients adopted to train the ANN coefficients, and the coefficients trained by ANN is shown in Figure 3a,b. Also, R2 coefficient is reported in such figures. Results show a poor dispersion. A good agreement between the coefficient forecasted by ANN and fitting on FE results is confirmed. As a matter of fact, concerning C1, the R2 is approximately 1. Looking at Figure 4 and Figure 5, it is possible to put in evidence that the R2 coefficient is always high. In particular, it never falls below 0.997.

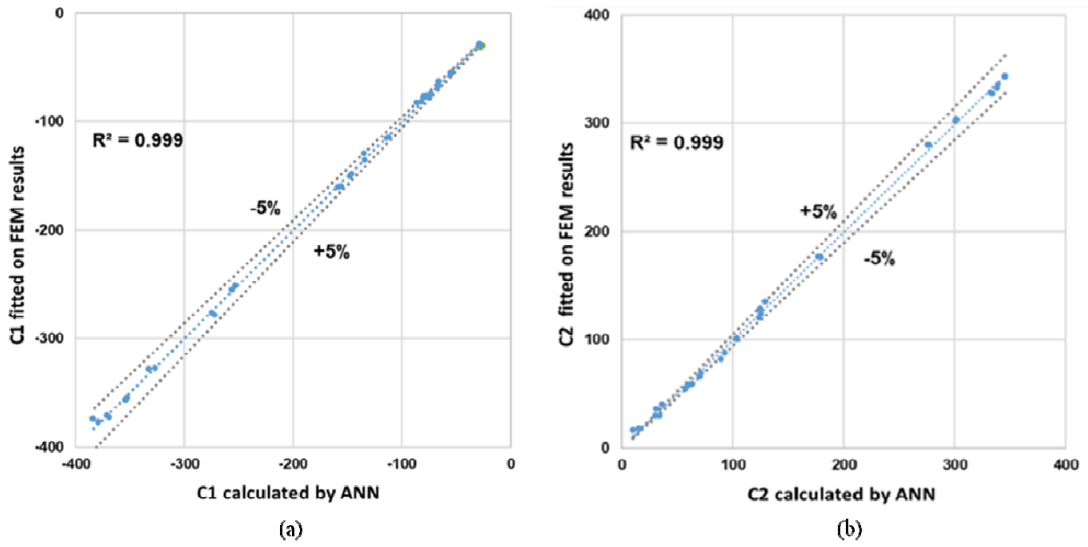

Figure 3. Plot of C1 from the analytical model C1 (target) versus the ANN trained C1 in blue with error bands at +5% and –5% in grey (a) and the analytical model C2 (target) versus the ANN trained C2 in blue with error bands at +5% and –5% in grey (b).

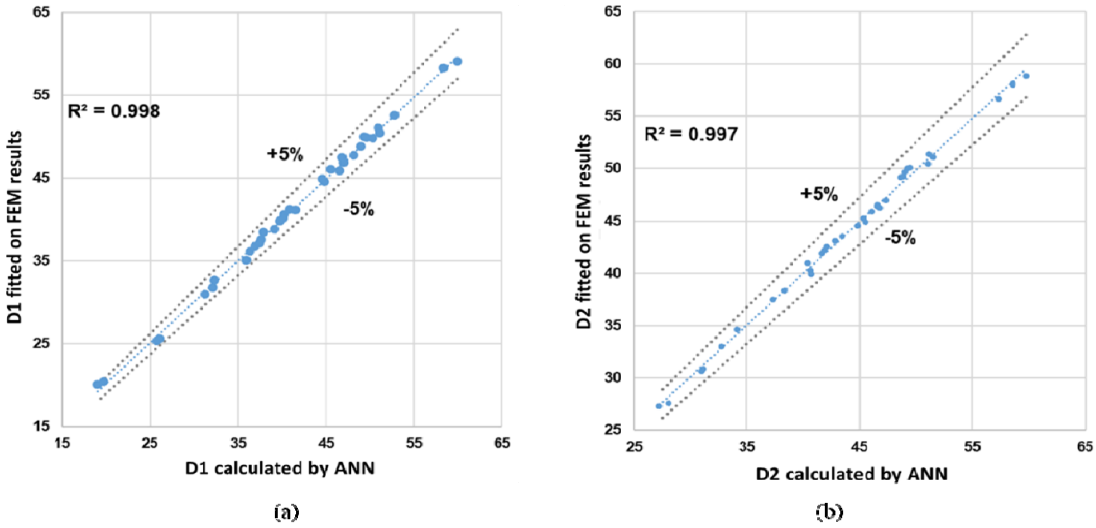

Figure 4. Plot of D1 from the analytical model D1 (target) versus the ANN trained D1 in blue with error bands at +5% and –5% in grey (a) and the analytical model D2 (target) versus the ANN trained D2 in blue with error bands at +5% and –5% in grey (b).

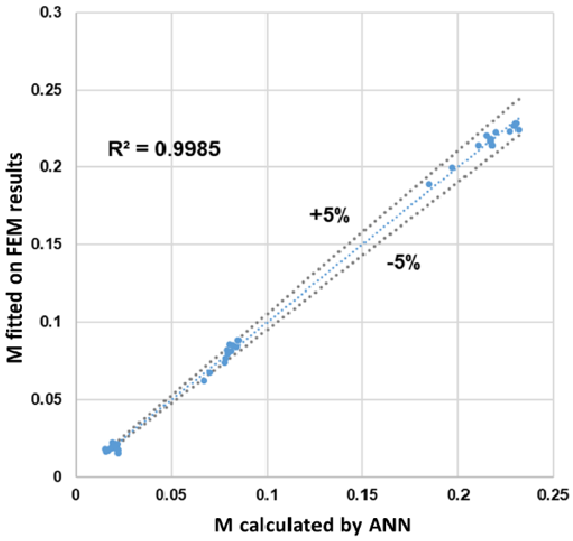

Figure 5. Plot of M from the analytical model M (target) versus the ANN trained M in blue with error bands at +5% and –5% in grey.

A comparison between FEM (black line), analytical model (as obtained by fitting of FEM data, red dot line) and analytical model with coeffects predicted by ANN (blue line) is reported in Figures 6–10 in terms of plastic strain dependence on arch length. The RMS deviation (green line) between the neural network and the analytical model results is also shown. The maximum RMS between the neural network and the analysis model is 14%. RMS curve shape (quite strict) is an indication of the consistency of the two approaches.

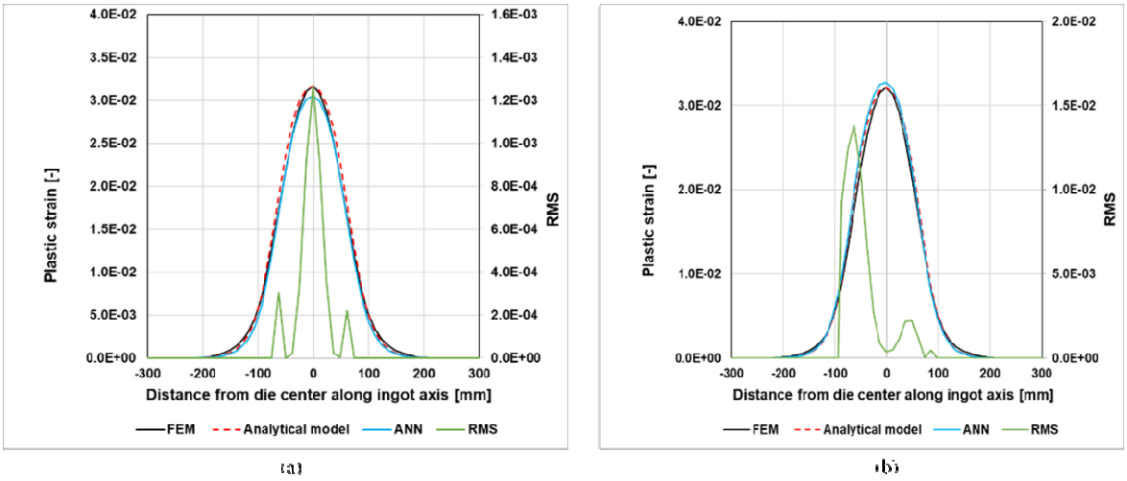

Figure 6. Total equivalent plastic strain as a function of length for Sb0 = 150mm, reduction of 5%, first stroke at (a) 800 °C, (b) 1200 °C.

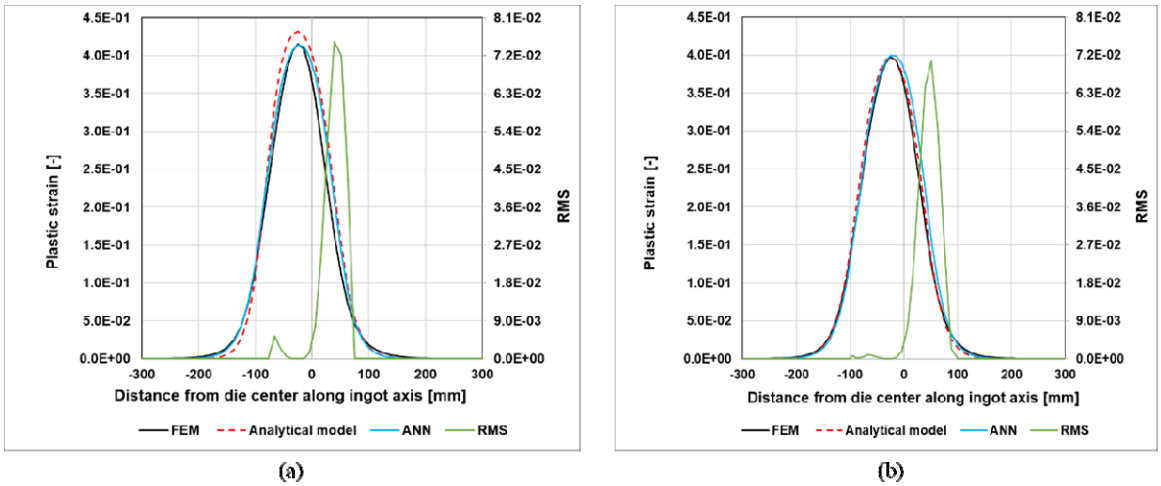

Figure 7. Total equivalent plastic strain as a function of length for Sb0 = 150mm, reduction of 25%, first stroke at (a) 800 °C, (b) 1200 °C.

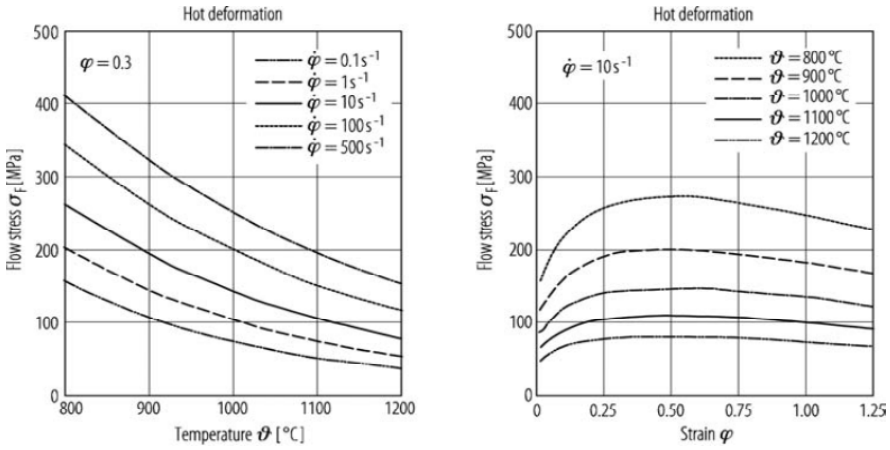

Figure 8. 42CrMo4. Flow stress curves by hot forming.

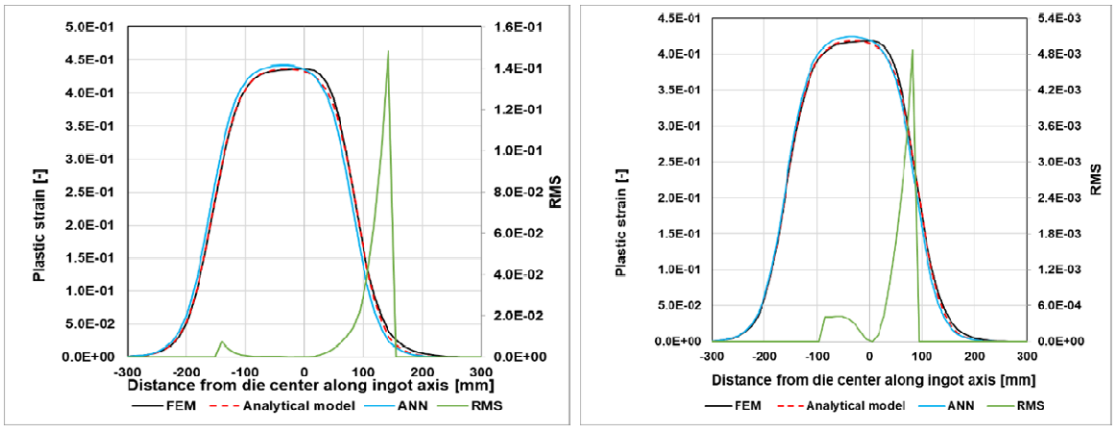

Figure 9. Total equivalent plastic strain as a function of length for Sb0 = 300mm, reduction of 25% for first stroke at (a) 800 °C, (b) 1200 °C.

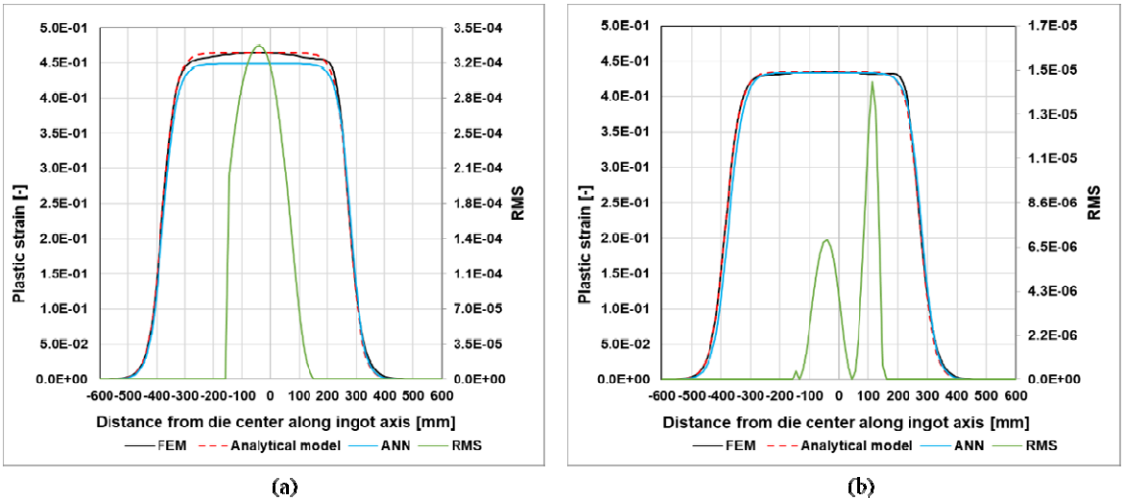

Figure 10. Total equivalent plastic strain as a function of length for Sb0 = 750mm, reduction of 25% for first stroke at (a) 800 °C, (b) 1200 °C.

The above comparison for the case corresponding to initial ingot diameter equal to 300 mm, Sb0 = 150 mm, reduction = 5% at 800 °C and 1200 °C is shown in Figure 6a,b, respectively. The proposed modeling approach provides the possibility to have two different slopes of the growth and decay phase of plastic strain (*e.g.,* different D1 and D2 coefficients). A similar behavior is reported in Figure 7, for the same initial ingot diameter and Sb0 = 150 mm. In this case higher reductions (25%) are considered. In this case two different temperatures (800 °C and 1200 °C) are compared. Figure 6 and Figure 7 show a very poor temperature variation of maximum plastic strain and shape of plastic strain on core fiber in the case of (Sb0 = 150 mm).

Differences on maximum plastic strain are equal to 1.4% and 4.4% for reduction rates of 5% and 25%, respectively, associated to a material softening from 800 to 1200 °C equal to 70% at strain = 0.3 and strain rate = 1 s^{-1} from 205 MPa to 62 MPa respectively (Figure 8). Such negligible rheological influence is related to isothermal hypothesis of FE forging modeling. Anyway, based on the above results, as a first approximation the proposed approach can be considered independent on the material properties.

Same conclusions can be drawn from Figures 9,10: in these cases, 800 °C and 1200 °C temperatures are considered for Sb0 = 300 mm and 750 mm, respectively. As Sb0 increases the maximum plastic deformation value on core fiber increases. In addition, a strong shift away from the growth and decay branches of plastic strain is observed as Sb0/D ratio increases. Also in this case a good agreement is found between the ANN approach and FEM results.

4. Conclusions

A hybrid approach is proposed in this paper, able to describe the plastic strain behavior at the core fiber of an open die forged round shape component. Such approach considers the following parameters: ingot diameter, die length Sb0, stroke reduction and deformation temperature. A rapid tool faster than the commonly used FEM method but with the same accuracy class is the result of such approach. This makes therefore it suitable for the rapid design of online forging processes. Results show that in the first approximation the material properties can be neglected. They become a

key issue when geometrical and metallurgical effects are also considered in the optimization model of forging. The described approach proposes therefore a rapid method aimed to design and optimize a forging open die process, thus allowing its adoption in industrial applications. In particular, differences on maximum plastic strain are equal to 1.4% and 4.4% for reduction rates of 5% and 25%, respectively, associated to a material softening from 800 to 1200 °C equal to 70% at strain = 0.3 and strain rate = 1 s^{-1} from 205 to 62 MPa respectively. Such negligible rheological influence is related to isothermal hypothesis of FE forging modeling. Anyway, based on the above results, as a first approximation the proposed approach can be considered independent on the material properties.

Conflict of interest

The author declares no conflict of interest.

References

1. Di Schino A (2020) Manufacturing and application of stainless steels. *Metals* 10: 327.
2. Pezzato L, Gennari C, Chukin D, et al. (2020) Study of the effect of multiple tempering in the impact toughness of forged S690 structural steel. *Metals* 10: 507.
3. Di Schino A, Di Nunzio PE, Lopez Turconi G (2007) Microstructure evolution during tempering of martensite in a medium-C steel. *Mater Sci Forum* 558: 1435–1441.
4. Dong D, Li H, Shan K, et al. (2018) Effects of different heat treatment process on mechanical properties and microstructure of Q690 steel plate. *IOP Conf Ser Mater Sci Eng* 394: 022017.
5. Di Schino A, Alleva L, Guagnelli M (2012) Microstructure evolution during quenching and tempering of martensite in a medium C steel. *Mater Sci Forum* 715–716: 860–865.
6. Algarni M (2019) Mechanical properties and microstructure characterization of AISI "D2" and "O1" cold work tool steels. *Metals* 9: 1169.
7. Rufini R, Di Pietro O, Di Schino A (2018) Predictive simulation of plastic processing of welded stainless steel pipes. *Metals* 8: 519.
8. Nakhaie D, Benhangi PH, Fazeli F, et al. (2012) Controlled forging of a Nb containing microalloyed steel for automotive applications. *Metall Mater Trans A* 43: 5209–5217.
9. Di Schino A, Kenny JM, Salvatori I, et al. (2001) Modelling primary recrystrallization and grain growth in a low nickel austenitic stainless steel. *J Mater Sci* 36: 593–601.
10. Shen G, Furrer D (2000) Manufacturing of aerospace forgings. *J Mat Process Tech* 8: 189–195.
11. Schafrik RE, Walsson S (2008) Challenges for high temperature materials in the new millennium, *Superalloys 2008-Proceedings of the 11th International Symposium on Superalloys*, 3–9.
12. Di Schino A (2017) Analysis of phase transformation in high strength low alloyed steels. *Metalurgija* 56: 349–352.
13. Dindorf R, Wos P (2020) Energy-saving hot open die forging process of heavy steel forgings on an industrial hydraulic forging press. *Energies* 13: 1620.
14. Di Schino A (2021) Microstructure and mechanical properties of forged steels. *Metals* 11: 32.
15. Di Schino A (2016) Analysis of heat treatment effect on microstructural features evolution in a micro-alloyed martensitic steel. *Acta Metall Slovaca* 22: 266–270.
16. Mancini S, Langellotto L, Di Nunzio PE, et al. (2020) Defect reduction and quality optimization by modelling plastic deformation and metallurgical evolution in ferritic stainless steels. *Metals* 10: 186.

17. Y Qiu, Park SC, Cho HY (2020) Prediction of forming limits in cold open-die extrusion process. *Trans Korean Soc Mech Eng A* 44: 435–441.
18. Harris N, Shahriari D, Jahazi M (2016) Analysis of void closure during open die forging process of large size steel ingots. *Key Eng Mater* 716: 579–585.
19. Di Schino A, Di Nunzio PE (2017) Metallurgical aspects related to contact fatigue phenomena in steels for back up rolling. *Acta Metall Slovaca* 23: 62–71.
20. Sharma DK, Filipponi M, Di Schino A, et al. (2019) Corrosion behavior of high temperature fuel cells: Issues for materials selection. *Metalurgija* 58: 347–351.
21. Di Schino A, Testani C (2020) Corrosion behavior and mechanical properties of AISI 216 stainless steel clad Q235 plate. *Metals* 10: 552.
22. Choi SK, Chun MS, Van Tyne CJ, et al. (2006) Optimization of open die forging of round shapes using FEM analysis. *J Mater Process Tech* 172: 88–95.
23. Obiko J, Mwema FM (2021) Stress and strain distribution in the upsetting process: A Numerical Simulation, In: Burstein L, *Handbook of Research on Advancements in Manufacturing, Materials, and Mechanical Engineering*, 288–301.
24. Rosenstoc D, Recker D, Hirt G, et al. (2013) Application of a fast calculation model for the process monitoring of open die forging processes. *Key Eng Mater* 554: 248–263.
25. Siemer E, Nieschwitz P, Kopp R (1986) Quality-optimized process control in open-die forging. *Stahl Und Eisen* 106: 383–387.
26. Napoli G, Di Schino A, Paura M, et al. (2018) Colouring titanium alloys by anodic oxidation. *Metalurgija* 57: 111–113.
27. Kim PH, Chun MS, Yi JJ, et al. (2002) Pass schedule algorithms for hot open die forging. *J Mater Process Tech* 130: 516–523.
28. Jarl M (2004) FEM simulation of drawing out in open die forging. *Steel Res Int* 75: 812–817.
29. Recker D, Franzke M, Hirt G (2011) Fast models for online optimization during open die forging. *CIRP Ann-Manuf Techn* 60: 295–298.
30. Franzke M, Recker D, Hirt G (2008) Development of a process model for online optimization of open die forging of large workpieces. *Steel Res Int* 79: 753–757.
31. Haykin S (1994) *Neural Networks: A Comprehensive Foundation*, 2 Eds., Ontario: McMaster University.
32. Russell S, Norvig P (2003) *Artificial Intelligence: A Modern Approach*, 2 Eds., Prentice Hall.
33. Hung C, Kobayashi S (1992) Three-dimensional finite element analysis on open-die block forging design. *J Eng Ind* 111: 459–464.
34. Skunca M, Skakun P, Keran Z, et al. (2006) Relations between numerical simulation and experiment in closed die forging of a gear. *J Mater Process Tech* 177: 256–260.
35. Zhang Z, Xie J (2006) A numerical simulation of super-plastic die forging process for Zr-based bulk metallic glass spur gear. *Mater Sci Eng A-Struct* 433: 323–328.
36. Hensel A, Spittel T (1978) *Kraft-und Arbeitsbedarf bildsamer Formgebungsverfahren*, Leipzig: VEB Deutscher Verlag für Grundstoffindustrie. (in German)
37. Shah KN, Kiefer BV, Gavigan JJ (1986) Finite element simulation of internal void closure in open-die press forging. *Mater Manuf Process* 1: 501–516.
38. Li YP, Matsumoto H, Chiba A (2009) Correcting the stress strain curve in the stroke-rate controlling forging process. *Metall Mater Trans A* 40: 1203–1209.
39. Caglar MU, Teufel AI, Wilke CO (2018) Sicegar: R package for sigmoidal and double-sigmoidal curve fitting. *PeerJ* 6: e4251.

40. Schlang M, Feldkeller B, Lang B, et al. (1999) Neural computation in steel industry. *1999 European Control Conference (ECC)* 2922–2927.
41. Di Schino A, Gaggiotti M, Testani C (2020) Heat treatment effect on microstructure evolution in a 7% Cr steel for forging. *Metals* 10: 808.
42. Wasserman PD (1993) *Advanced Methods in Neural Computing*, New York: John Wiley & Sons.

AIMS Press